Biogeosciences
Discussions

Lawns and meadows in urban green space - A comparison from greenhouse gas, drought resilience and biodiversity perspectives

Justine Trémeau[1,2,3,4], Beñat Olascoaga[4,5,6], Leif Backman[1], Esko Karvinen[1], Henriikka Vekuri[1] and Liisa Kulmala[1,7]

5   [1] Finnish Meteorological Institute, Helsinki, Finland
    [2] AgroParisTech – Institut des sciences et industries du vivant et de l'environnement, Palaiseau, France
    [3] Université Paris-Saclay, Orsay, France
    [4] Institute for Atmospheric and Earth System Research (INAR), Department of Physics, Faculty of Science, University of Helsinki, Helsinki, Finland
10 [5] School of Resource Wisdom, Department of Biological and Environmental Science, Faculty of Mathematics and Science, University of Jyväskylä, Jyväskylä, Finland
    [6] Helsinki Institute of Sustainability Science (HELSUS), Department of Forest Sciences, Faculty of Agriculture and Forestry, University of Helsinki, Helsinki, Finland
    [7] Institute for Atmospheric and Earth System Research (INAR), Forest Sciences, University of Helsinki, Helsinki, Finland

15

Correspondence: Justine Trémeau (justine.tremeau@fmi.fi) and Liisa Kulmala (liisa.kulmala@fmi.fi)

Abstract. Nowadays, city planners design urban futures by considering climate change and biodiversity loss. Here, we studied the greenhouse gas fluxes of urban lawns and meadows and linked the observations with plant functional diversity and soil properties. CO_2, CH_4 and N_2O fluxes, as well as plant diversity, were measured in eight lawn–meadow pairs in the
20 Helsinki Metropolitan Area, Finland. Among the sites, an irrigated lawn, a non-irrigated lawn, a young dry meadow and an old mesic meadow were intensively studied especially using manual chamber measurements in 2021–2022. The process-based ecosystem model JSBACH was utilized together with the momentary observations on CO_2 exchange to quantify the annual C balance of these intensive study sites. On another hand, the initial dynamics of conversion from lawns to meadows were studied with the six other pairs, where measurements were conducted from 2020 to 2022 and the transformation of half
25 of the sites had been performed in late 2020. We found that lawns are clear sink of carbon, whereas the mesic meadow was more resistant to drought events than a non-irrigated lawn. Moreover, according to our results, the conversion from lawn to meadow did not affect the fluxes of CH_4 and N_2O. Last, the relation between C and N cycle and plant diversity was unclear and would need further investigations.

30 **Keywords.** carbon balance, photosynthesis, respiration, CH4, N2O, JSBACH, plant diversity, urban nature

1 Introduction

The impacts of climate change and biodiversity crises are increasingly evident. The crises have feedbacks with each other as climate change threatens biodiversity, and the loss of biodiversity and possible degradation of ecosystems affects the climate system. Therefore, it is crucial to understand the role that various ecosystems in the land-use sector play in regulating climate
35 and supporting biodiversity, and to find land management practices that can effectively mitigate the climate and biodiversity crises simultaneously. Such well-known management practices for the land use sector include, for example, conservation and restoration, and integrated land-use planning taking into account the relationships between different land uses (Pörtner et al., 2021).

Species richness can affect carbon sequestration potential in several ways. Generally, ecosystems with higher species
40 richness are shown to have higher photosynthetic productivity than less diverse systems, because of the more efficient use of resources by the greater variety of species contributing to carbon uptake (Fornara and Tilman, 2008; Lange et al., 2015; Yang et al., 2019; Chen et al., 2020). In addition, increased species richness can lead to a more resistant functioning of the

ecosystem in extreme weather events, as the responses by different species can respond differently to changes in environmental conditions (De Keersmaecker et al., 2016; Hossain et al., 2022). This means that, for example, during a

45 drought some species may be more resistant, making the functioning of a diverse ecosystem less vulnerable compared to a habitat with lower species richness. However, the relationship between species richness, productivity and resistance is not straightforward, but influenced by many factors, such as ecosystem management, species cortege and environmental conditions (Vogel et al., 2012; De Keersmaecker et al., 2016; Jung et al., 2020).

Urban green spaces provide vital ecosystem services, such as cooling, recreation, purification of air and water, and risk

50 reduction for flooding (Belmeziti et al., 2018; Lampinen et al., 2021). Cities actively seek optimal green area planning and management practices to mitigate and adapt to climate change and there are also numerous initiatives aimed at promoting urban green spaces and infrastructure. One of those is Article 6 in the Nature restoration proposal launched by the European Commission (European Commission, 2022), which sets targets for increasing green urban spaces in cities, towns and suburbs.

55 Within urban landscapes, lawns constitute one of the most common features of the green space, and are usually subjected to frequent and intense mowing regimes to fulfil social, aesthetic and recreational purposes. Although many types of lawns exist, most of the urban green spaces worldwide are dominated by turfgrass lawn. These lawns typically contain certain selected species, yet they can also harbor other species of forbs and grasses that are spontaneously established, thus giving lawns the ability to behave like semi-natural grasslands (Thompson et al., 2004; Fischer et al., 2013). Reducing the

60 conventional turfgrass lawn management has proved to enhance the abundance, species richness and diversity of vegetation and arthropods (Venn and Kotze, 2014; Watson et al., 2020), thus leading these passively created urban grasslands to have a positive effect on biodiversity. An alternative approach to creating more environmentally friendly and biodiverse urban grasslands consists of substituting or modifying part of the lawnscape from the short, monocultural, homogeneous setting of grass species into a flowering setting with extensive management and active incorporation of forbs (Southon et al., 2017;

65 Lane et al., 2019; Norton et al., 2019; Bretzel et al., 2020). This practice is becoming increasingly common as more cities and other communities look for ways to create sustainable and low-maintenance green space (Norton et al., 2019). However, the relative impact of urban lawns and meadows, and the transformation between them, on soil and vegetation dynamics, carbon balance and greenhouse gas (GHG) exchange, remains poorly understood.

70 The aim of this study is to determine the climatic impact of transforming urban lawns into meadows in northern Europe. In practise, we had four specific research questions:

1. Does the carbon balance differ between urban lawns and meadows?
2. Are meadows more tolerant to extreme weather events than lawns?
3. Does the transformation from lawn to meadow increase GHG emissions?
75 4. Does plant diversity affect GHG fluxes?

In addition, we were interested to see if we could detect any connections between diversity and C and N pools. To answer these questions, we measured GHG fluxes in urban lawns, recently created meadows and an older urban meadow in a more advanced phase around the Helsinki Metropolitan Area in Finland. Observations of the sites were used to set up a land-surface model, which was used to simulate annual carbon balances forced by reanalysis data. The empirical data set included

80 intensive sites with high temporal coverage and satellite sites with high spatial coverage.

2 Materials and method

2.1 Site description

2.1.1 Study region

The measurements were collected within the Helsinki Metropolitan Area (60°10' N, 24°57' E, Fig. 1), which is situated on
85   the northern coast of the Gulf of Finland. In Helsinki, the mean annual precipitation and temperature were 653 mm and 6.5 °C, respectively, for the reference period of 1991–2020, with monthly mean temperatures being above 10 °C from May to September (Jokinen et al., 2021). According to the Köppen climate classification, the climate is humid continental (Dfb) (Kottek et al., 2006).

2.1.2 Intensive sites

90   Two pairs of lawns and meadows, situated 4 kilometers apart, were selected for the intensive measurement sites (Fig. 1). In Kumpula (KMP) neighborhood, an old and mesic meadow was paired with a highly managed lawn situated 150 meters away inside the Kumpula botanical garden. The meadow is an old agricultural field on which farming practices were abandoned about 40 years ago. Nowadays, *Aegopodium podagraria*, *Lupinus polyphyllus*, *Dactylis glomerata*, *Anthriscus sylvestris*, *Elymus repens*, *Lamium album* and *Urtica dioica* are the dominant species. It is cut once a year in autumn and most of the
95   vegetation clippings are taken away. It is neither irrigated nor fertilized. The lawn, mainly covered by *Poa pratensis*, was installed about 15 years ago. It is currently mowed automatically by a mowing robot that operates daily between 6 PM and 11 AM, and the grass clippings are pounded and left on the site. It is irrigated during the summer when needed and was last fertilized in spring 2021.

In Viikki (VKI) neighborhood, the lawn and meadow are situated inside a public park 60 meters apart from each other. The
100 lawn of *Festuca sp.* was sown in 2005 and is managed as a "utility lawn" (Viherympäristöliitto, 2023). It is mown regularly so that the grass height is 4–12 cm, and the clippings are mostly left on the site. There is no irrigation, and the lawn has not been fertilized for several years. A section of the park's lawns was transformed into a dry meadow in 2020 by replacing the topsoil with a layer of recycled sand and sowing seeds (Riikonen and Karilas, 2021). In 2022, the dominant species were *Trifolium repens*, *Tripleurospermum inodorum*, *Lecanthemum vulgare*, *Centaurea jacea*, *Phleum pratense* and *Plantago*
105 *major*, and some rare species such as *Dianthus deltoides*, *Campanula rotundifolia* and *Galium verum* were also observed. It was fertilized in spring 2021 and mown for the first time in autumn 2022. Most of the clippings were removed from the site.

2.1.3 Satellite sites

Six locations belonging to local student housing associations were selected for high spatial coverage GHG measurements in the urban green space. In each of the locations, 50 m^2 of an already established lawn was transformed into an urban meadow
110 site by volunteering and community participation.

Site transformations were conducted during late autumn 2020 by manually turning over the existent soil up to a depth of ca. 35 cm, followed by the sowing of 14 pollinator-friendly forbs at a density of 0.7 g m^{-2}. The commercial seed mixture (Suomen niittysiemen Oy, Koski Tl, Finland) also included four grass species at a density up to 0.7 g m^{-2}. Consequently, the hemiparasitic forb *Rhinanthus minor*, which has shown to have negative effects on grass cover (Chaudron et al., 2021), was
115 sown at a 6 g m^{-2} density.

Every year since the lawn transformation, each of the developing urban meadows was managed by manually removing on-site tree seedlings (mainly *Acer platanoides*) before a one-time mowing event in autumn by hand scythe. Lastly, all mowing clippings were removed from the sites. Six urban lawns over 20 years old, each located nearby the developing urban meadows and all subject to regular lawn management, were selected and studied as control cases. All of the six lawns were
120 predominantly covered by *Poaceae* sp.
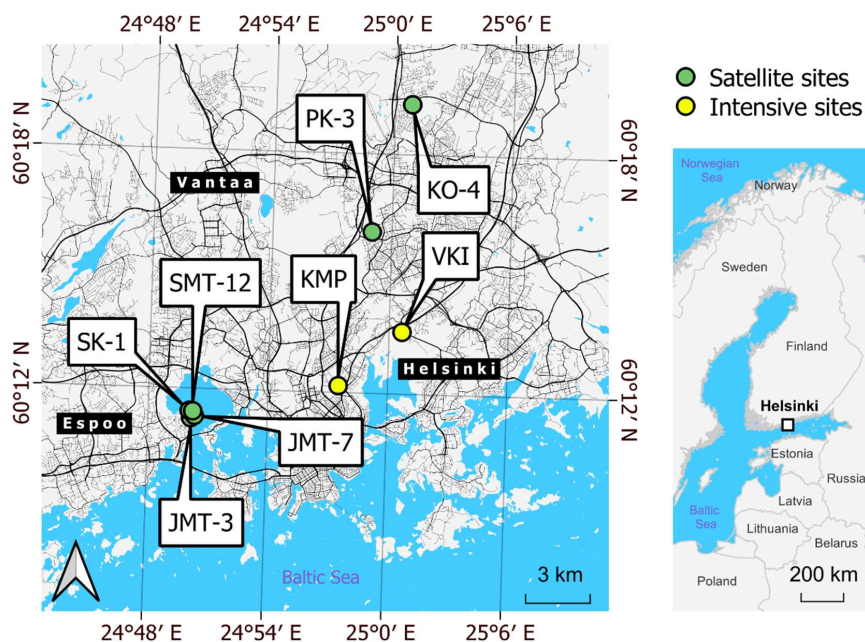
Figure 1. Locations of the intensive (yellow) and satellite measurement sites (green) around the Helsinki metropolitan area.
125 **Background maps built with topographic database by National Land Survey of Finland (2023) and global administrative borders by GADM (2023).**

Table 1. Site characteristics at the intensive and satellite sites. Sown mixture indicates seeds of pollinator-friendly forbs, grass species and *Rhinanthus minor* which were sown in late 2020.

Site ID	Experiment	Management	Soil texture	Type of vegetation	Irrigation	Sand (%)	Silt (%)	Clay (%)	pH	SOC (%)	SON (%)	CN ratio
VKI lawn	intensive	lawn	sandy loam	Fescue	No	72.2	25.6	2.2	6.3	2.8	0.19	14.5
VKI meadow	intensive	meadow	sandy loam	Xerophilic	No	72.4	17.1	10.5	6.1	2.5	0.17	14.9
KMP lawn	intensive	lawn	sandy loam	Poa	Yes	69.5	22.1	8.4	5.6	3.8	0.25	14.8
KMP meadow	intensive	meadow	sandy loam	Mesic	No	59.1	31.8	9.1	6.5	5.6	0.46	12.3
JMT3C	satellite	lawn	silt loam	Poa	No	5.2	68.9	26.0	5.3	5.0	0.46	10.8
JMT3T	satellite	meadow	loamy sand	Sown mixture	No	73.7	23.5	2.8	6.5	4.6	0.18	25.7
JMT7C	satellite	lawn	loamy sand	Poa	No	82.7	14.9	2.4	6.5	4.0	0.26	15.0
JMT7T	satellite	meadow	loamy sand	Sown mixture	No	81.4	16.0	2.6	6.5	3.2	0.21	15.3
KO4C	satellite	lawn	sandy loam	Poa	No	66.2	29.4	4.4	6.4	4.4	0.29	15.4
KO4T	satellite	meadow	sandy loam	Sown mixture	No	63.3	32.7	4.0	6.1	4.0	0.19	20.9
PK3C	satellite	lawn	sandy loam	Poa	No	68.8	27.6	3.6	6.2	4.0	0.19	21.1
PK3T	satellite	meadow	sandy loam	Sown mixture	No	68.4	27.1	4.5	6.1	5.4	0.32	17.2
SK1C	satellite	lawn	sandy loam	Poa	No	57.3	33.9	8.8	5.6	4.5	0.37	12.3
SK1T	satellite	meadow	sandy loam	Sown mixture	No	54.1	36.5	9.4	5.4	4.2	0.35	12.0
SMT12C	satellite	lawn	loam	Poa	No	47.7	42.7	9.7	5.8	3.6	0.29	12.8
SMT12T	satellite	meadow	loam	Sown mixture	No	51.8	39.6	8.6	6.1	4.4	0.31	14.2

130

2.2 Flux measurements

2.2.1 Measurement protocol

The GHG flux measurements were conducted with manual chambers with different setups at the intensive and satellite sites. At the intensive sites, the CO_2 exchange measurements were conducted more often than in the satellite sites, and they also included the light response (LR) of net ecosystem exchange (NEE). At the satellite sites, the measurements also included CH_4 and N_2O exchanges, but measurements were conducted with opaque chambers, thus disabling photosynthesis.

At the intensive sites, the light response of NEE was measured fortnightly between June and September 2021–2022. Additional measurements of NEE, but mainly of total ecosystem respiration (TER), were also conducted in May and in October–November. The measurement setup consisted of a transparent chamber attached to a CO_2 and H_2O analyzer (Li-840A, LI-COR, Inc., Nebraska, USA), an air temperature and humidity sensor (BME280, Bosch Sensortec GmbH, Reutlingen, Germany), and a photosynthetically active radiation (PAR) sensor (PQS1, Kipp & Zonen, Delft, Netherlands). The air was circulated through the analyzer at a flow rate of 1 L min^{-1}, and the chamber was equipped with a small fan to ensure air mixing within the chamber headspace. We used two differently sized chambers, either 0.072 m^3 or 0.288 m^3, and three collars of different heights (18.3 cm, 20.8 cm and 50 cm) to individually match the height of the chamber+collar combination to the vegetation we were measuring during each measurement day. Chamber measurements were performed on four fixed plots established on the lawn and the meadow at each of the two locations. At VKI lawn and meadow as well as at KMP meadow, the plots were located about 10 meters apart, along a single diagonal transect. The plots on KMP lawn were located in two separate transects 15 meters away from each other, with the two plots on each transect being 3 meters apart.

The transparent chamber was placed on the ground while avoiding damaging the plants, and a tight seal was created by using sand-filled cloth bags as insulation. In meadows, when a collar was used, it was placed on the ground and sealed with the cloth bags, and the chamber was placed on top of the collar. The duration of each chamber closure was at least 2 minutes. To determine the light response of NEE, we repeated the measurement five times at each plot under different PAR intensities created by shading the chamber with netted or opaque fabrics. We first measured without covering the chamber and then covered it with 1–3 layers of mesh cloth. Eventually, we measured with an opaque cover. The chamber was kept well-ventilated between measurements. We allowed for ±10% variation in the PAR level during a single closure. TER was obtained from the measurement conducted with the opaque cover.

At the satellite sites, GHG measurements were conducted with a dark chamber monthly, between May–September 2021–2022. Additional background measurements were conducted in July, August and October 2020, before the lawn transformations took place. The measurement setup in August and October 2020, as well as in May, July and September 2021 and 2022 consisted of a CO_2, H_2O, N_2O and CH_4 analyzer (DX4015, Gasmet Technologies Oy, Vantaa, Finland) connected to an opaque chamber equipped with a small fan. The chamber volume was either 0.00456 m^3 or 0.268 m^3 depending on the height of the vegetation measured. An additional collar of 20 cm height was needed to allow enough room for tall vegetation in July 2021 and 2022. The measurements in July 2020 and in June and August in 2021 and 2022 were conducted with a setup consisting of an opaque chamber (volume 0.007434 m^3) equipped with a CO_2 probe (GMP343, Vaisala Oyj, Vantaa, Finland), a relative humidity and air temperature sensor (HMP75, Vaisala), and a small fan. This chamber is introduced in detail by Ryhti et al. (2021). Four study plots were established both on the lawn and the meadow at each of the six locations. From the centroid of the site, a 10 m long transect was established along the length of the site, with four quadrats of 1 m^2 area each uniformly distributed, and the chamber measurements were always performed within these quadrats. When measuring only CO_2 (i.e., July 2020, June and August 2021 and 2022), the duration of each chamber closure was 4–5 minutes. We extended the closure time to 15 minutes when measuring also N_2O and CH_4 (i.e., May, July and September).

Soil temperature and soil moisture were always measured together with the chamber measurements at both the intensive and the satellite sites. One replicate of soil temperature was measured next to each flux measurement plot at a 10 cm depth with a
175   handheld soil thermometer (HH376, Omega Engineering Inc., Connecticut, USA), and 4–5 replicates of soil moisture at 5 cm depth were measured with a handheld setup (ML3 ThetaProbe and HH2 Moisture Meter, Delta-T Devices Ltd., Cambridge, UK). All plots were also photographed from above on each measurement day to calculate the green cover percentage of the basal area within the chamber using Canopeo (Patrignani and Ochsner, 2015).

2.2.2 Flux calculation

180   The measurement represents the total ecosystem fluxes: total CH_4 fluxes (gCH_4 m^{-2} s^{-1}), total N_2O fluxes (gN_2O m^{-2} s^{-1}) and NEE (gCO_2 m^{-2} s^{-1}). NEE includes possible photosynthetic input (GPP, gCO_2 m^{-2} s^{-1}) and the outflow by respiration (TER, gCO_2 m^{-2} s^{-1}), which includes both autotrophic and heterotrophic respiration. This can be mathematically written as:

$$NEE(t) = TER(t) + GPP(PAR(t)),   \qquad (1)$$

where PAR (µmol m^{-2} s^{-1}) is photosynthetically active radiation and t is time. Here we use meteorological notation i.e., we
185   consider the inflow of carbon to be negative (GPP≤0) and therefore NEE can be either negative (i.e., sink of CO_2), when the absolute value of GPP is higher than TER, or positive (i.e., source), when TER is higher than the absolute value of GPP.

NEE or the total flux of other GHG fluxes during each chamber closure was calculated with the following Equation (2):

$$flux = \left(\frac{dC(t)}{dt}\right)_{t=0} \frac{M_{GHG}\, P\, V}{R\, T\, A},   \qquad (2)$$

where $\left(\frac{dC(t)}{dt}\right)_{t=0}$ is the time derivative (ppm s^{-1} = 10^{-6} s^{-1}) of the linear regression, M_{GHG} is the molecular mass of the GHG
190   (44.01 g mol^{-1} for CO_2, 16.05 g mol^{-1} for CH_4 and 44.02 g mol^{-1} for N_2O), P is the air pressure (Pa), V is the system (chamber + possible collar) volume (m^3), R is the universal gas constant (8.31446 J mol^{-1} K^{-1}), T is the mean temperature inside the chamber headspace during the closure (K) and A is the soil surface i.e. the basal area of the chamber (m^2).

To ensure a proper air mixing inside the chamber, at least ten seconds were removed from the beginning of each closure
195   before fitting a linear regression into the GHG concentration values. Otherwise, the quality control and the length of the measurements included in the flux calculations differed between the instruments and GHGs. For the Vaisala equipment, CO_2 fluxes were calculated with the first minute of the recordings with R (version 4.2.2) after visual validation of linearity. Python (version 3.9.7) was used to calculate the fluxes measured by the two other devices. With the Gasmet analyzer, the CO_2 fluxes were calculated from the first five minutes of the recordings whereas CH_4 and N_2O fluxes, which were
200   significantly lower fluxes and closer to the detection limits of the equipment, were calculated with the first seven minutes of the recordings. For the intensive sites, where the LI-COR analyzer was used, all fluxes were calculated from at least the first minute of the recording. There, possible poor-quality measurements were eliminated from the end of the measurement period if there was at least 1 minute of good quality data. The quality control measures were stability of light conditions inside the chamber during the closure and normalized root mean squared error (NRMSE) of the fit. Varying light conditions during the
205   closure were inspected by calculating the standard deviation of PAR. If the standard deviation was larger than 150 µmol m^{-2} s^{-1} during the closure, the measurement was discarded. Yet, it is worth noting that in cases where the flux is nearly zero, NRMSE can be very large even though the measurement is not erroneous. Therefore, we did not discard measurements based on NRMSE if $(\frac{dC(t)}{dt})_{t=0}$ was below 0.1 ppm s^{-1}. Otherwise, measurements were discarded if NRMSE was larger than 0.05. Accordingly, 41 NEE measurements out of 1225 recordings were discarded from the intensive site dataset, but none of
210   them referred to the opaque chamber measurements, i.e., TER. Thus, TER was represented by 23 and 20 days of data at KMP and VKI sites, respectively. Regarding the satellite sites, no fluxes were discarded.

2.2.3 Light response (LR) fitting and daily GPP

In order to fit LR curves to the CO_2 flux data, we first subtracted TER from the other NEE rates to obtain an estimate for GPP (Eq. 1). GPP(PAR=0) was set to zero. The LR curve was expected to be a rectangular hyperbola (Ruimy et al., 1995),

215 as follows:

$$GPP = \frac{PAR\, \alpha\, GPmax}{PAR\, \alpha + GPmax},$$ (3)

where PAR (μmol m^{-2} s^{-1}) is photosynthetically active radiation, α (mg μmol^{-1}) is the initial slope between GPP and PAR, and GPmax (mgCO$_2$ m^{-2} s^{-1}) is the light-saturated photosynthesis rate. The parameters α and GPmax were estimated using non-linear least squares minimization. α was allowed to vary between -0.1 and $-1*10^{-8}$ mg μmol^{-1} and GPmax between -5

220 and $-1*10^{-7}$ mgCO$_2$ m^{-2} s^{-1}.

After processing the light response calculation, LR curves where α had standard error over 0.0008 mg μmol^{-1} or GPmax was higher than 10 mgCO$_2$ m^{-2} s^{-1} were discarded from the dataset. In addition, LR was discarded if the highest PAR intensity in the response was under 500 μmol m^{-2} s^{-1}. That resulted in 154 LR curves out of 212, representing 14 days of data at KMP meadow, VKI lawn and meadow and 10 days at KMP lawn, which were used in further analyses.

225

Daily GPP was calculated for each plot and for each measurement day using Eq. 3, fitted parameters for the plot and day, and continuous PAR measurements from SMEAR III station (Institute of Atmospheric Research, 2023). First, GPP was estimated for each half hour with the fitted parameters and the 30 min average PAR. Then, all half-hourly GPPs were summed up to obtain the daily GPP of the plot on the particular day.

230 2.3 Soil sampling

The overall soil characteristics at the intensive sites were analyzed at a commercial lab (Eurofins Viljavuuspalvelu Oy, Mikkeli, Finland). We collected altogether 1 L of soil up to 25 cm depth at each of the sites. At KMP lawn, the pooled sample comprised of 16–18 individual samples systematically collected around the site with a thin auger (d = 2.3 cm). At the rest of the remaining intensive sites, we used a slightly larger auger (d = 5.0 cm) to collect 4 individual samples that were

235 then pooled together. The fresh samples were stored in a fridge and sent to the lab within 1–3 days after collection. The particle size distribution was analyzed according to Elonen (1971).

Soil density samples were collected by digging a small pit and carefully inserting a steel cylinder (V = 0.151 dm^3) horizontally into an undisturbed pit wall at 10 cm depth. When the cylinder was fully inserted, it was gently detached by removing the surrounding soil while ensuring that all soil within the cylinder remained in place in order to achieve

240 volumetric accuracy. Five replicates were collected at KMP lawn and 3 replicates at the other intensive sites. After collection, the samples were dried at 105 °C for 48 h and the dry weights were weighed.

At KMP sites, samples for C and N were collected with an auger (d = 2.3 cm) down to a 30 cm depth. Altogether, six individual samples were collected systematically at the lawn and the meadow. At VKI, we used an auger (d = 1.7 cm) to collect eight samples and then pooled them together. The fresh samples were sieved (mesh size = 2 mm) and the fresh

245 weights of the smaller and larger soil fractions were weighed. The soil was dried at 105 °C for 24 h. Total soil C and N contents were determined from dried and milled samples of soil smaller than 2 mm with an elemental CN analyzer (LECO, Michigan, USA).

All soil samples from the satellite sites were collected during early July 2022, and all samples were extracted within a 1 m^2 radius from the plots in which GHG fluxes were measured. A total of four soil cores, dug by means of a soil auger of 5 cm

250 diameter down to ca. 15 cm depth, were pooled together to create a composite soil sample. In each of the sites, a total of four composite soil samples were collected in ziplock bags and kept on ice during soil collection. All soil samples were then stored at −20 °C, until shipped and analyzed at a commercial lab (Eurofins Viljavuuspalvelu Oy, Mikkeli, Finland). Total

soil C and N contents were determined from freeze-dried and milled samples with an elemental CN analyzer (LECO, Michigan, USA). For the case of soil particle size distribution, a fraction of each of the soil samples was repeatedly washed

255 with a 30% H_2O_2 solution to remove its organic matter content. The resulting soil samples were then dried out at 105 °C for 48 h, before sieving (mesh size = 0.6 mm) the final mineral soils. The sieved soil samples were then mixed with a sodium pyrophosphate solution (0.05 M), and their sand, silt and clay proportions were calculated by means of laser diffraction particle size analyzer (Bekman Coulter LS230, Beckman Coulter Inc., California, USA).

2.4 Biodiversity inventory

260 Vegetation inventories were conducted in all intensive and satellite sites. Four quadrats of 1 m^2 each were distributed along the transects, in the same location as the chamber measurements. In each of the quadrats, the cover of each plant species was estimated and classified in one of the following categories: forb, grass, horsetail, legume, moss, sedge or tree. Species richness (*S*) was estimated at site-level, considering all grass species to be a combined, singular entity. Site species richness was used for the estimation of the site's Shannon diversity index value (*H'*), as Equation (4):

265 $$H' = -\sum_{i=1}^{S} p_i ln(p_i) ,$$ (4)

where p_i is the proportion of cover related to the ith species, and *S* is the number of species in the site.

Lastly, species evenness (*E*) at the site was calculated as, Equation (5):

$$E = \frac{H'}{\ln(S)} .$$ (5)

2.5 Ecosystem modelling

270 The intensive sites were simulated using the JSBACH, which is the land model in the Earth system models of the Max-Planck Institute for Meteorology (Reick et al., 2013). The model was driven with hourly data of air temperature, precipitation, shortwave and longwave radiation, relative humidity and wind speed. The driver data were derived from observations from the Kumpula weather station (60°12'1".1" N, 24°57'4".7" E) operated by the Finnish Meteorological Institute. The data was gapfilled by observations from the nearby urban measurement station SMEAR III (Järvi et al., 2009).

275 Hourly ERA5-Land data (Muñoz-Sabater et al., 2021) were used to fill a small number of remaining gaps. Leaf area index (LAI) data for the simulated sites were obtained from Sentinel-2 satellite data (Nevalainen et al., 2022; Nevalainen, 2022).

The vegetation in JSBACH is represented by plant functional types (PFT). The model was set up for simulating only one PFT, C3 grass, for each site. The Logistic Growth Phenology (LoGro-P) model (Böttcher et al., 2016) is used to describe the phenology in JSBACH, where the temporal development of the leaf area index (LAI) of grass depends on both temperature

280 and soil moisture. The maximum LAI for each site (Table S2) was set based on Sentinel-2 data (Nevalainen et al., 2022; Nevalainen, 2022). In addition, in the simulation of the Kumpula meadow the shedding of the grass was activated 65 days after the growth started, in order to better follow the observed LAI.

According to the soil particle size distribution the soil texture at all sites was sandy loam. The parameters describing the soil properties follow the recommendations by Hagemann and Stacke (2015). However, the volumetric field capacity and wilting

285 point for each site were adjusted based on the soil moisture measurements (Table S2). The root depths of the lawns were assumed to be shallower than for the meadows (Table S2).

The photosynthesis of C3-plants in JSBACH is described by the model by Farquhar et al. (1980). The photosynthesis is calculated once to get the unstressed canopy conductance, which is then scaled based on the soil moisture in the root zone to get the canopy conductance and photosynthesis under water stress. The available water in the roots zone depends on the field

290 capacity, root depth and a scaling factor f=(W-Wwilt)/(Wcrit-Wwilt). The scaling factor is applied for relative soil moisture values between Wcrit=fcrit*Wmax and Wwilt=fwilt*Wmax, where Wmax is the maximum moisture content in the root

zone. No water is available to the vegetation when the soil moisture reaches fwilt*Wmax. The factors fcrit and fwilt are given in Table S2.

The adjusted model, forced with the observed weather, was used to derive the annual average GPP, TER and NEE of the
295   intensive sites (KMP, VKI) for the period 2005–2021.

2.6 Study of drought events

2.6.1 Drought definition

Since drought could be defined by the deficit of precipitation and the increase in evaporation (Wang et al., 2021), we estimated the drought period at our intensive sites with the Standardized Precipitation-Evapotranspiration Index (SPEI). We
300   calculated the drought period at a 14-day scale with the SPEI R package (Vicente-Serrano et al., 2010; Beguería et al., 2014). The Penman equation was used to calculate the Potential Evapotranspiration (PET) with the method of the FAO. The altitude was fixed at 10 m and the latitude at 60°11' N.

The minimum temperature, maximum temperature, wind speed, cloud amount, dew point temperature, relative humidity and air pressure, all collected at an hourly scale and averaged at a daily level, were downloaded from the Finnish Meteorological
305   Database at the Kumpula meteorological station (Finnish Meteorological Institute, 2023).

The drought periods were weekly defined with SPEI under −1.5, corresponding to the highest value describing a severe drought (Wang et al., 2021): a week with at least one daily SPEI value under −1.5 was considered as a drought week.

2.6.2 Statistical analyses regarding drought stress

With the collected data, the resilience of the different grassland habitats to drought events was estimated. As resilience is the
310   result of both components resistance and recovery, we studied in this paper only the resistance, which was defined as "the magnitude of disturbance that a system can absorb before shifting from one state to another" (Capdevila et al., 2021).

Thus, to estimate the direct impact of drought on lawns and meadows, we chose to primarily compare KMP meadow and VKI lawn, since both of these habitats were older than 15 years and non-irrigated. In addition, we also included KMP lawn in the comparison to see the effect of irrigation. The yearly summer means of TER, daily GPP, green cover, soil temperature
315   and soil moisture were calculated for each site, by considering that the summer season starts on week number 22 and ends on week number 34 (data collected from May 31st–August 24th 2021 and June 3rd–August 25th 2022). Lastly, we calculated the differences between the measured values of the variable and the summer average of the same variable at the site level. These calculated differences were then normalized at a site and year level by subtracting the annual means of the differences and dividing the whole by the annual standard deviation of the differences.

320   With the summer data, we defined two categories: data collected during the drought events and data collected outside of the drought events. Finally, with Mann-Whitney U tests, we compared, pair by pair, VKI lawn, KMP lawn and KMP meadow in the different summer conditions.

2.7 Statistical analyses at the satellite sites

2.7.1 Dynamics of GHG fluxes

325   All statistical analyses were run using R (version 4.2.2). Shapiro-Wilk tests were used to evaluate the normal distribution of each variable by year and type (meadow vs. lawn). Then, differences in given variables between lawns and meadows were assessed either by t-tests or Mann-Whitney U tests depending on the normality of the data.

2.7.2 Statistical analyses of plant variable contribution

The effects of plant diversity and vegetation functional categories on SOC, SON and GHG fluxes were studied in all
330   intensive and satellite sites with the plant and fluxes data collected in 2022. The fluxes were averaged for the growing
season, from May to September. The effects of vegetation were assessed by applying linear mixed-effects models (LMMs),
using the R lme4 package (Bates et al., 2015), where the factor "location" was included as a random effect. 18 mixed-effect
linear regressions were built using one by one each of the biodiversity indices (i.e., species richness, Shannon index and
species evenness) as predictive variables and each of the GHG fluxes as well as SOC and SON values as response variables.
335   To test the contribution of each plant functional category on the GHG fluxes, as well as on SOC and SON values, 6 mixed-
effect multiple regressions including the proportions of all plant functional categories (i.e., legumes, grasses, forbs, trees
(saplings), sedges, horsetails and mosses) as predictive variables were run by applying a descending selection. At each
iteration, predictive variables with p-values higher than 0.1 were removed and variables with p-values lower than 0.05 were
considered statistically significant. Before testing any regression, the distributions of each of the LMMs were visually
340   checked with Quantile-Quantile (Q-Q) plots and a conditional R-squared was used to assess the quality of the model.

3 Results

3.1 Drought occurrences

There was 7% and 12% more precipitation in 2021 and 2022 compared to the 653 mm-value of the reference period 1991–
2020 (Jokinen et al., 2021), but in both years July was drier than the long term average, with 17% and 15% less precipitation
345   in 2021 and 2022 respectively (47 mm in 2021 and 49 mm in 2022 compared to 57 mm in 1991–2020). At the same time,
2021 and 2022 were 0.1 and 0.4 °C warmer than the reference which was 6.5 °C. The summers were on average hotter than
the reference period with 2.5 °C and 1.8 °C higher temperatures in 2021 and 2022, respectively, compared to 16.6 °C. These
particularly hot and dry weeks were observed from June 14th to August 1st 2021 and from June 6th to July 17th 2022 (Fig. 2a).
At the intensive sites, the measured soil moisture (Fig. 2b) also showed a drastic decrease at all sites during these two
350   periods, except at the irrigated KMP lawn, where the soil moisture remained relatively high during the whole summer. The
highest soil temperature was also reached during the same period (Fig. 2c). In 2021 and 2022, those hot and dry weeks also
corresponded to the decrease phase of LAI, except at VKI meadow, where LAI increased slowly from spring until August
(Fig. 2d). The measured green cover was notably following the same patterns as the satellite LAI data (Fig. 2e).
With the SPEI, two drought periods were defined: the first one from June 14th to August 8th in 2021, and the second one from
355   June 27th to July 17th in 2022 (Fig. 2). Thus, the defined drought event in 2021 happened early in the summer season and
lasted eight weeks, whereas the drought event in 2022 arrived later in the summer and lasted only three weeks. These two
drought events co-occurred with the high temperature and low soil moisture periods described above.

360
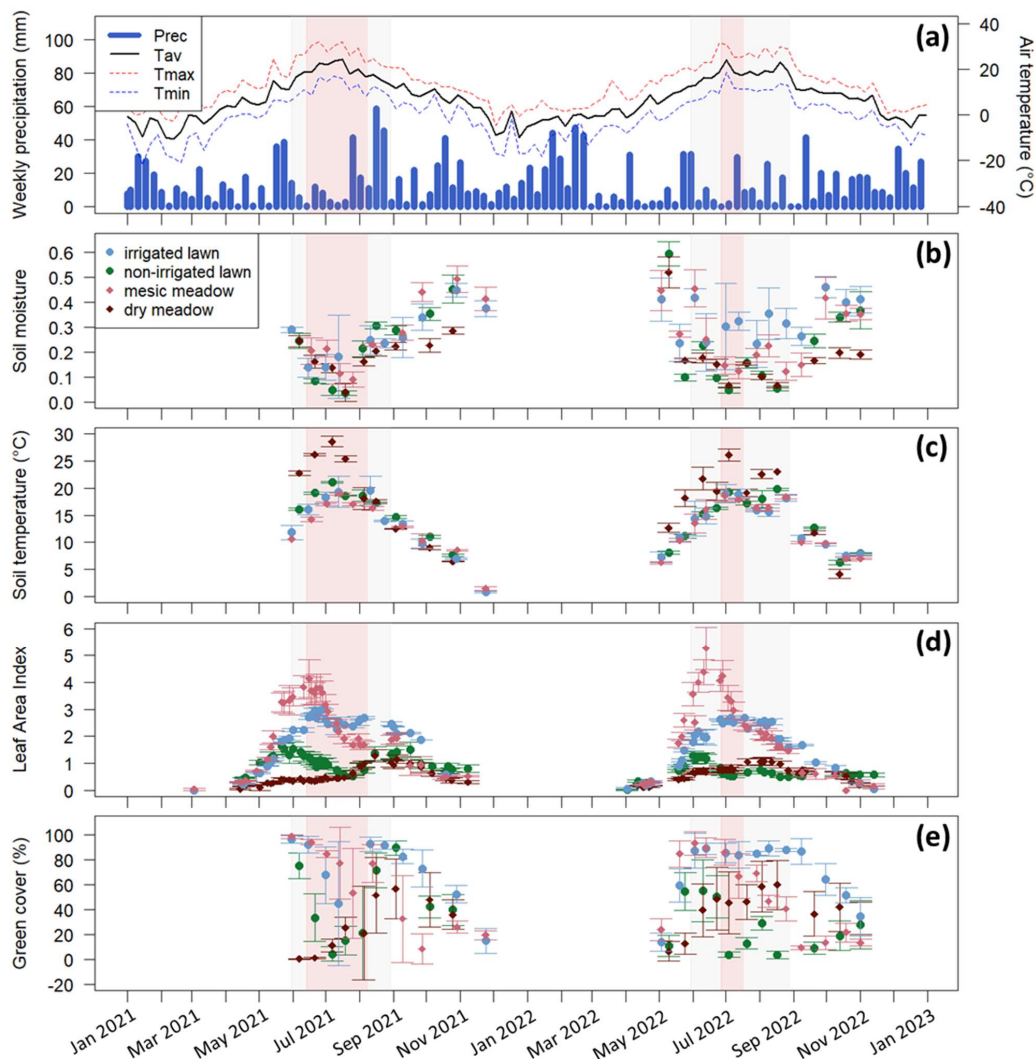
Figure 2. Weekly precipitation (Prec.) and mean air temperature (Tav) recorded by FMI meteorology station (a), manually measured soil moisture at a 5 cm depth (b), manually measured soil temperature at a 10 cm depth (c), leaf area index from satellite Sentinel-2 (d) and manually measured green cover (e) at the intensive study sites with standard deviations during the campaign
365 **years 2021–2022. The irrigated lawn is KMP lawn, the non-irrigated lawn is VKI lawn, the mesic meadow is KMP meadow, and the dry meadow is VKI meadow. Red rectangles indicate the drought periods according to the SPEI and light grey rectangles represent the summer season. In panel (a), Tmax and Tmin represent the weekly instantaneous maximum and minimum mean temperatures.**

3.2 CO₂ fluxes

370 **3.2.1 Observed seasonal variation**

At all intensive sites, the measured TER increased at the beginning of the measurement campaign and declined during the drought events at the non-irrigated sites (Figure 3 and S1). When comparing the differences between the four sites, the mean momentary TER was the highest at KMP meadow (0.44 and 0.31 mgCO$_2$ m^{-2} s^{-1} in 2021 and 2022, respectively) and the lowest at VKI meadow (0.29 and 0.26 mgCO$_2$ m^{-2} s^{-1} in 2021 and 2022, respectively). The highest recorded mean values

375 (0.86, 0.84, 0.59, 0.59 mgCO$_2$ m^{-2} s^{-1}) were measured at VKI lawn, KMP meadow, VKI meadow, KMP lawn, on June 7th,

July 2nd, July 19th, August 11th, respectively, in 2021. In 2022, the highest values (0.71, 0.49, 0.65, 0.55 mgCO$_2$ m^{-2} s^{-1}) were recorded at VKI meadow, KMP lawn, KMP meadow, VKI lawn on June 23rd, June 30th, July 1st, August 17th, respectively. In general, daily TER were higher at KMP sites compared with VKI sites, although the highest values were not reached in a specific order.

380 There were site-specific variations in the seasonal pattern of GPP (Figure S1). In the first campaign year, after the first measurements, the daily GPP sink decreased at all sites except VKI meadow, for which it was the first growing season after establishment. In 2022, the daily GPP sinks first increased and then started to decrease around the end of June (Figure 3). The highest recorded daily uptakes (−0.48, −0.51, −0.40, −0.46 mgCO$_2$ m^{-2} s^{-1}) were measured at VKI lawn, KMP meadow, VKI meadow, KMP lawn, on June 7th, June 18th, August 5th, August 11th, respectively, in 2021. In 2022, the order had also

385 slightly changed as the highest uptakes (−0.37, −0.58, −0.42 and −0.47 mgCO$_2$ m^{-2} s^{-1}) were recorded at VKI lawn, KMP meadow, KMP lawn, VKI meadow on June 10th, June 13th, June 13th and June 23rd. Thus, the measured GPP values were higher at KMP sites than at VKI sites.

3.2.2 JSBACH performance

The simulated soil moisture (Fig. S2) varied according to irrigation, precipitation and evaporation and showed lower values

390 in summer, particularly in June and July, and also in August in 2022. The modelled seasonal dynamics in soil moisture followed the observations in general; however, some of the observations were considered to represent moisture content above the volumetric field capacity. The soil moisture in the model is limited by the field capacity (Fig. S2). At the same time, the modelled soil temperature between 10 and 15 cm depth agreed with the measured soil temperature at 10 cm depth (Fig S3). Modelled LAI varied in accordance with the observations especially at KMP meadow and on the second year at

395 VKI meadow (Fig. S4). For VKI meadow, the drought response was not captured in the model simulation in early summer 2021 during the first growing season of the meadow. The drought response for VKI lawn agreed with the observations in 2021, while in 2022 the recovery was too strong in the simulation. At KMP lawn, the simulated LAI decreased later in 2022 than the observed LAI (Fig. S4).

Simulated TER fits the observations at KMP lawn in 2021–2022 and at KMP meadow in 2022 (Fig. 3, Fig. S5). The

400 measured instantaneous TER was sometimes higher than modelled TER in summer, while it overlapped with the modelled TER in spring and in autumn (Fig. 3 and S5). Simulated daily mean GPP followed the observations closely (Fig. 3), except at VKI meadow where the model overestimated the observations in early season after the sowing (Fig. S5h), which is probably due to the discrepancy in LAI between the simulation and observations.

3.2.3 Annual balances

405 During 2005–2021, simulated annual GPP and TER were on average the highest at KMP lawn and meadow (Table 2). GPP and TER were the lowest at VKI meadow (Table 2) being approximately 40% of those of KMP lawn and meadow. The unirrigated lawn GPP and TER was approximately 70% of those of irrigated lawn. The lawns resulted on average in more negative NEE i.e., a greater sink of carbon, than meadows, and looking at the ratio between standard deviation and NEE, meadows showed higher year-to-year variations than the lawns (Table 2). The sink of the irrigated lawn (KMP lawn) was

410 approximately 53% higher than that of the unirrigated lawn (VKI lawn).
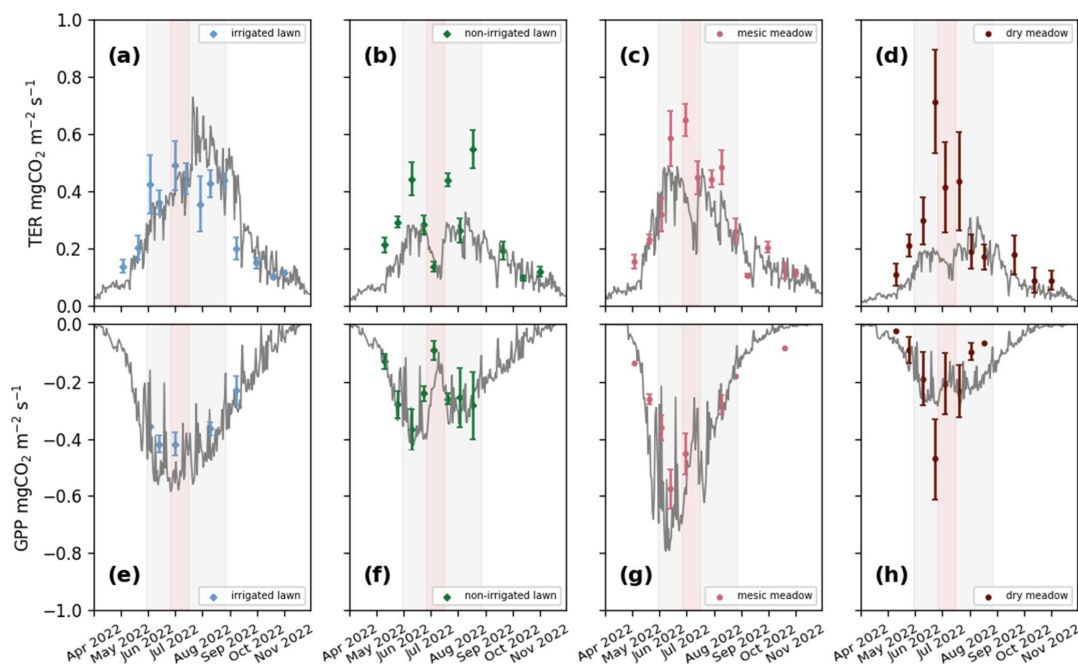
Figure 3. Seasonal dynamics of mean total ecosystem respiration (TER, abcd) and daily photosynthesis (GPP, efgh) in the four intensive sites in 2022. Grey continuous lines represent JSBACH simulations and diamonds and dots represent the mean of manual measurements with standard deviation bars. (a, e) Irrigated lawn = KMP lawn; (b, f) non-irrigated lawn = VKI lawn; (c, g) mesic meadow = KMP meadow; (d, h) dry meadow = VKI meadow. Red rectangles indicate the drought periods according to the SPEI and light grey rectangles represent the summer season.

Table 2. Mean annual (± standard deviations calculated for 2005–2022) of ecosystem respiration (TER), photosynthetic uptake (GPP) and net ecosystem exchange (NEE) modeled with JSBACH at the four intensive sites during the years 2005–2022.

Sites	Characteristics	TER (gCO$_2$ m^{-2} y^{-1})	GPP (gCO$_2$ m^{-2} y^{-1})	NEE (gCO$_2$ m^{-2} y^{-1})
KMP lawn	Irrigated lawn	4331 (± 177)	−4667 (± 218)	−336 (± 187)
VKI lawn	Non-irrigated lawn	3039 (± 251)	−3196 (± 231)	−157 (± 139)
KMP meadow	Mesic meadow	4127 (± 291)	−4278 (± 233)	−151 (± 198)
VKI meadow	Dry meadow	1765 (± 136)	−1828 (± 161)	−63 (± 134)

### 3.3 Extreme weather resistance

Green cover, TER and daily GPP were significantly decreased at the unirrigated lawn (VKI lawn) compared to the records outside the drought and to the mature meadow (KMP meadow) and the irrigated lawn (KMP lawn) during the prolonged drought in 2021 (Fig. 4ace) and during the shorter drought in 2022 (Fig. 4bdf). In 2022, TER was significantly higher at the irrigated lawn and at the mesic meadow during the drought than outside of the drought period (Fig. 4d).
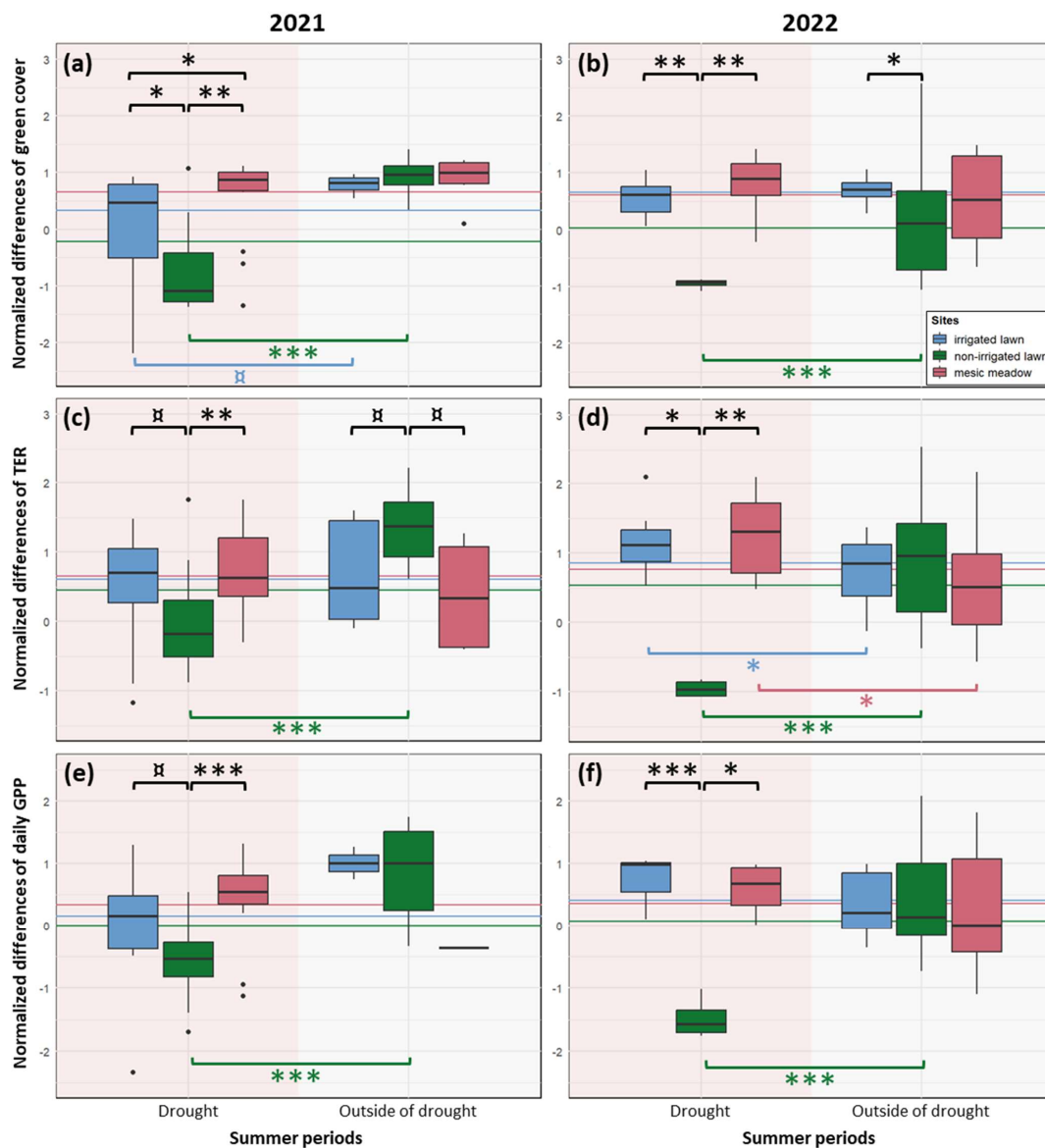
Figure 4. The resistance indices of an irrigated lawn (KMP lawn), a non-irrigated lawn (VKI lawn) and an old mesic urban meadow (KMP meadow) to drought events in 2021 (first column) and 2022 (second column), calculated for the green cover (a, b), the TER (c, d) and the daily GPP converted to positive values (e, f). The values are the differences between the measured values and the summer average, normalized at a yearly level. Horizontal lines represent the normalized summer means of each site. Summer includes Jun–Aug and droughts were defined in Fig. 2 (June 14th–August 8th, 2021 and June 27th–July 17th, 2022). (¤ for p-value ≤ 0.10; * for p-value ≤ 0.05; ** for p-value ≤ 0.01; and *** for p-value ≤ 0.001).

3.4 CH₄ and N₂O fluxes
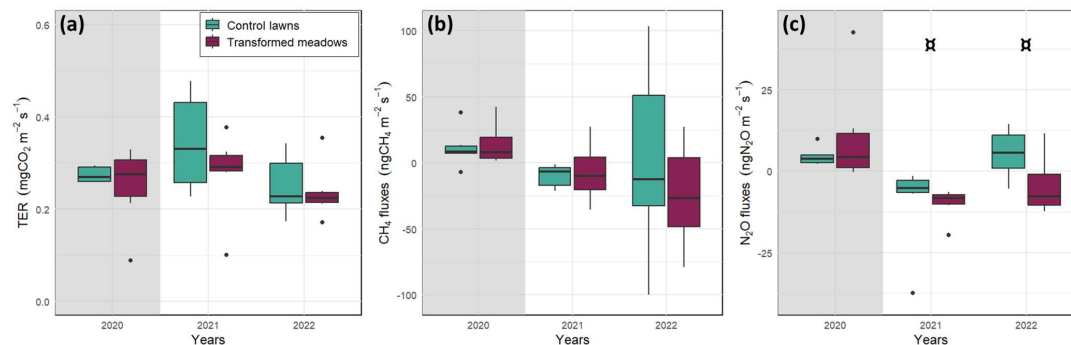
Figure 5. Box and whisker plots of measured (a) total ecosystem respiration (TER), (b) CH₄ and (c) N₂O fluxes of lawns and
440 **transformed meadows at the satellite sites before (grey background) and after transformation (white background), which**
happened in the end of 2020 only at the transformed meadows. Statistical differences between both types of green spaces were
tested at the year level (¤ for p-value ≤ 0.10; and * for p-value ≤ 0.05).

At the satellite sites, before the transformation in 2020, there were no differences between lawn and meadow sites in terms of
445 TER, CH₄ and N₂O fluxes measured in darkened conditions (Fig. 5). There was some general year-to-year variation in the
median and range of observed CO_2 and CH₄ fluxes, but the fluxes did not differ between lawns and transformed meadows in
2021 or 2022 (p > 0.1, Fig. 5ab). The mean N₂O fluxes were slightly lower in meadows than in lawns in 2021 and 2022 (p-
value < 0.1, Fig. 5c). Soil moisture and temperature did not differ between the treatments during the measurements (Fig. S7).

3.5 Biotic predictor variables for C and N cycles

450 According to the linear regressions, TER, CH₄ fluxes, N₂O fluxes, SOC, SON and C/N ratio were not related with species
richness, Shannon index, nor Species evenness according to the data collected in 2022 (Table 3).

With the six multiple regressions, we found that TER was positively related with almost all vegetation categories, except
mosses and just with minor significance positively with sedges and trees, and negatively with horsetails (Table 4). CH₄
appeared to be significantly and negatively correlated with sedges and positively with horsetails (Table 4), and N₂O was
455 mainly negatively associated with forbs and positively with horsetails (Table 4). SOC was slightly positively explained by
forbs proportion whereas SON appeared to be significantly positively connected with grass proportions and almost with
forbs (Table 4). The C/N ratio was significantly and negatively connected with legume, grass and forb proportions (Table 4).

Table 3. Effect of plant diversity (i.e., species richness, Shannon index and species evenness) on total ecosystem respiration of CO₂
460 **(TER), CH₄ fluxes, N₂O fluxes, Soil C content (SOC), Soil N content (SON) and C/N ratio. ((p-value) for p-value > 0.05; * for p-**
value ≤ 0.05; ** for p-value ≤ 0.01; and * for p-value ≤ 0.001). ˢᵃᵗ· indicates values that were only measured at satellite sites.**

	Predictive variables					
	Species richness		Shannon index		Species evenness	
Response variables	Estimate	R-squared	Estimate	R-squared	Estimate	R-squared
TER (mgCO₂ m⁻² s⁻¹)	−0.001 (0.60)	0.70	−0.02 (0.22)	0.73	−0.08 (0.16)	0.74
CH₄ fluxes (ngCH₄ m⁻² s⁻¹) ˢᵃᵗ·	−3.35 (0.42)	0.29	−26.27 (0.38)	0.28	−73.13 (0.46)	0.27
N₂O fluxes (ngN₂O m⁻² s⁻¹) ˢᵃᵗ·	−0.24 (0.75)	0.009	−7.52 (0.14)	0.19	−29.16 (0.08)	0.32
SOC (%, < 2 mm)	0.05 (0.29)	0.36	0.38 (0.24)	0.40	1.17 (0.28)	0.40
SON (%, < 2 mm)	0.0001 (0.98)	0.00003	−0.01 (0.81)	0.004	−0.04 (0.77)	0.005
C/N ratio	0.23 (0.34)	0.06	2.51 (0.14)	0.14	8.46 (0.12)	0.18

Table 4. The connection between the proportions of different plant functional categories and total ecosystem respiration of CO_2 (TER), CH_4 fluxes, N_2O fluxes, Soil C content (SOC), Soil N content (SON) and C/N ratio. The plant functional categories are legumes (*Fabaceae*), grasses (*Poaceae*), forbs (other families of flowering vascular plants, which do not belong to one of the listed categories), trees, sedges (*Carex*), horsetails (*Equisetum*), and mosses (*Bryophyta*). (NS for p-value > 0.10; ◻ for p-value ≤ 0.10; * for p-value ≤ 0.05; ** for p-value ≤ 0.01; and * for p-value ≤ 0.001). sat. indicates values that were only measured at satellite sites.**

Response variables	Predictive variables							R-squared
	Legumes	Grasses	Forbs	Trees	Sedges	Horsetails	Mosses	
TER ($mgCO_2$ m^{-2} s^{-1})	0.003 *	0.002 **	0.001*	0.063 ◻	17.658 ◻	−0.297 ◻	NS	0.92
CH_4 fluxes ($ngCH_4$ m^{-2} s^{-1}) sat.	NS	NS	NS	NS	−22039.32 *	366.476 *	2.429 ◻	0.77
N_2O fluxes (ngN_2O m^{-2} s^{-1}) sat.	0.585 ◻	NS	−0.278 **	NS	NS	1.087 **	NS	0.98
SOC (%, < 2 mm)	NS	NS	0.011 ◻	NS	NS	NS	NS	0.56
SON (%, < 2 mm)	NS	0.002 *	0.002 ◻	NS	NS	NS	NS	0.28
C/N ratio	−0.281 **	−0.159 ***	−0.079 **	NS	NS	NS	NS	0.69

4 Discussion

It is well known that converting lawns into meadows can increase biodiversity in cities (Venn and Kotze, 2014; Wastian et al., 2016; Chollet et al., 2018). In this study, we wanted to understand better how transforming lawns into meadows in nordic urban areas could affect their GHG fluxes and how their vegetation diversity could influence the C and N cycles. The studied sites, an irrigated lawn, a non-irrigated lawn, an old mesic spontaneous meadow and a young dry meadow, were mainly C sinks. Moreover, with a focus on the transformation dynamic from lawns into meadows, no significant differences in measured GHG fluxes (CO_2, CH_4 and N_2O) were found between the six control sites and six transformed sites in the two following years after the conversion. However, the studied mesic meadow appeared to be more resistant to drought stress than unirrigated lawn. This resistance could notably be explained by plant diversity, as discussed later. Furthermore, even though some further studies would be necessary to understand better the interaction between the plants and the C and N cycles, we found that the mixture of plants functional categories showed some links with the C and N cycle.

4.1 Fluxes in urban grasslands

Carbon neutrality is nowadays one of the major goals for cities and states in mitigating climate change (IPCC, 2022). Our aim was to understand how CO_2 sequestration differs between lawns and meadows by studying contrasting habitats, a very fertile and a very poor meadow together with irrigated and non-irrigated lawns, to determine the full range of the exchange. We found that the photosynthetic production (GPP) of an irrigated lawn and a mesic meadow roughly equaled on an annual scale whereas the GPP of a non-irrigated lawn was notably lower. The irrigation increased the GPP of a lawn by over 40% and the sink (NEE) by more than 100%. It has already been found that water input improves carbon uptakes (Thienelt and Anderson, 2021) and demonstrated by Zirkle et al. (2011) that irrigated lawns store up to 10 gC m^{-2} y^{-1} more carbon in soil than non-irrigated ones, whereas our study indicated as much as approximately 50 gC m^{-2} y^{-1} higher sink on an irrigated lawn.

Here, the model estimates for NEE had some uncertainties as the model was unable to simulate some of the observed momentary total ecosystem respiration (TER) values during summertime (Fig. 3) which caused the full carbon balance estimate to be more uncertain than the estimated GPP. In this experiment, we were measuring the plots at various times of day due to practical reasons, even though Pavelka et al. (2018) suggest measuring ecosystem respiration in the morning around 9–10 to get the average level of daily respiration. Moreover, with manual chamber measurements, we were able to measure only once or twice a month and most of the time under a sunny weather, whereas with automatic chambers or eddy

495 covariance (Hiller et al., 2011; Thienelt and Anderson, 2021), it would have been possible to estimate the daily and monthly variations at a finer scale and to reduce the bias caused by hot and dry days. Therefore, especially during the summertime, the measured values most probably are overestimations of the daily average whereas in the early spring and in autumn, when the diurnal cycle in soil temperature and plant activity are smaller, the observations fit the model estimate nicely. Last, it has been shown that during cold days, under snow and/or frozen ground, grasslands are a source of CO_2 (Hiller et al., 2011). The

500 highest ecosystem activities and emissions take place in the warm summer months but to fully validate the annual balance, it would be useful to have some wintertime observations as well. On the other hand, we can be quite confident in the simulated photosynthetic production, since GPP principally occurs during the snow-free seasons.

All our sites were estimated to be small sinks of carbon varying between 63–336 gCO_2 m^{-2} y^{-1} whereas the results of earlier studies are conflicting. Many have reported urban grasslands to be C sources (Bezyk et al., 2018; Hundertmark et al., 2021)

505 but others have also reported sinks of about 20–180 gCO_2 m^{-2} y^{-1} (Thienelt and Anderson, 2021). We found that lawns were stronger sinks than the meadows which is in line with Peoplau et al. (2016) who found that that soil C was higher in lawns than in meadows, which was mainly attributed to the clippings left at the site and fertilization.

It is noteworthy that lawns in Finland have a certain requirement for soil fertility whereas meadows grow on various types of soil ranging from poor and dry to mesic and fertile. We found that the mesic meadow, with high (max. 1.3 m) and dense

510 vegetation in summer, had higher photosynthetic production and annual sink than the dry meadow sown late 2020. However, during the campaign the dry meadow was still in an initial phase i.e., its carbon sequestration potential may not have been fully realized, with about six-times lower CO_2 uptake than the mesic meadow. In addition, in the same meadow, there were dissimilar features among the four sampled plots: one of them was scarce in plants, another one had a tall and dense vegetation, and the two others had a short dense vegetation, which have made the model fitting and the analysis even more

515 challenging. For these reasons, it would be useful to compare in the future the fertile site to naturally dry and homogenous meadows with similar age.

Nevertheless here, we particularly focused on the transformation process with the satellite sites and found no negative climate impacts in terms of greenhouse gases during the campaign which covered two growing seasons after the transformation. However, it is possible that we missed some peaks of emissions as the measuring frequency was just once a

520 month. Nevertheless, it is quite safe to conclude that even if such unmonitored peaks occurred, their significance on an annual level would be minor as there was no indication of any differences during the measurements. On the other hand, it is evident that destroying vegetation during the transformation process decreases photosynthetic input at least during the following autumn and spring when lawns continue photosynthetic activities but when the new meadow has not developed yet. Therefore, it would have been interesting to measure GPP as well and conduct the experiment over a longer period of

525 time, as it has been shown that even grassland restoration requires of many more years (Muller et al., 1998; Waldén and Lindborg, 2016; Kose et al., 2021). In addition, the CO_2, H_2O, N_2O and CH_4 analyzer used at the satellite sites has a low sensitivity for small fluxes, at least in certain conditions (Kohl et al., 2019), in comparison with more advanced analyzers. However, we were only interested in the possible difference between the two treatments and not the actual rates nor annual balances and therefore, we find the choice to be acceptable. In any case, it would be important to study the CH_4 exchange, N

530 cycle and particularly N_2O fluxes in urban grasslands in more detail.

Finally, even though the spectra of our four intensive sites was wide, the four sites were unique in their environmental conditions, vegetation and management. In order to provide a stronger categorization, it would have been beneficial to study more replicates intensively. Moreover, mowing frequency was not studied, nor its carbon footprint, although studies have found notable impacts on source and sink due to managements (Allaire et al., 2008; Poeplau et al., 2016; Lerman and

535 Contosta, 2019; Thienelt and Anderson, 2021) leaving room for improvements for further studies.

Biogeosciences
Discussions

4.2 CO₂ fluxes impacted by drought events

Extreme climate events may occur more often in the coming years and during the two years of measurements in this study, dry summers impacted the ecosystems. Here, we focus only on the resistance component, i.e. the capacity of the system to absorb the drought disturbance during the event (Vogel et al., 2012; Capdevila et al., 2021). According to the comparison

540 between drought and the outside-of-drought periods, the unirrigated lawn reached a more desiccated stage during the dry period of the summer, whereas the meadows seemed to endure the deficit of water and the hot weather as well as the irrigated lawn. In unirrigated lawns, such a suppression is a physiological reaction to drought stress reducing photosynthesis (GPP) and respiration (TER), as also found in other studies (Allaire et al., 2008; Hiller et al., 2011; Vogel et al., 2012). Yet, it has been also demonstrated in several studies that species-rich grasslands better endure extreme weather events (Vogel et

545 al., 2012; De Keersmaecker et al., 2016).

The greater resistance of meadows compared to non-irrigated lawns could be explained by several factors, such as plant complementarity, microclimate and management (Vogel et al., 2012; De Keersmaecker et al., 2016; Bernath-Plaisted et al., 2023). (1) Lawns are usually sown, weeded and managed in order to maintain the desired low species composition and aesthetic appeal; on the other hand, plant diversity is usually much richer in meadows. Yet, the *samplings effect* theory

550 (Tilman et al., 1997; Loreau and Hector, 2001) argues that in a more diverse grassland, there is more chance to find at least one species, which is well adapted to drier habitats. For this reason, there is a higher chance for at least one plant species to survive during drought events in meadows than in lawns. (2) The second theory is the *niche complementarity*, which results from niche differentiations and the benefits of interspecific interactions among them (Tilman et al., 1997), and induces a better individual species performance (Tilman et al., 1997; Loreau and Hector, 2001). Such a high diversity of plants and

555 niches, as we can find in meadows, leads to a better water-use efficiency as described by De Boeck et al. (2006), and helps to face water shortage. In relation to (1) and (2), meadows usually contain vegetation with deeper root systems, which allow plant individuals to supply themselves with water and reduce competition for the available water in the upper soil layers during drought periods. (3) Moreover, this complementarity in meadows is reinforced by microclimate anomalies (Bernath-Plaisted et al., 2023). The tall and dense vegetation of meadows creates a buffer to face climate extreme events by offering

560 shade to the lower layers and keeping the humidity beneath the meadow canopy. (4) Finally, management, and notably mowing frequency, is also described as one of the factors impacting drought resistance. Regrowth of vegetation is more sensitive to extreme weather stress than vegetation at a later stage of its growth dynamics (Vogel et al., 2012). Hence, lawns are more affected, since they are typically mown every two to three weeks during the growing season, whereas meadows are cut one to two times a year. Thus, vegetated urban meadows are able to function almost as well as irrigated lawns and as

565 well as during regular summertime weather since, e.g., during and outside drought periods, the green cover and the photosynthetic uptake are comparable.

In this study, we did not have a reference year without a drought as according to daily SPEI calculation, both years of measurements were affected by extreme drought stress. Further, it would be important to understand how these ecosystems function during a normal climate year even though the pre-drought reference and post-drought stable stages used in this

570 study would better estimate the resistance itself (Capdevila et al., 2021), especially in 2021 when the drought period covered 8 weeks out of 13 weeks of summer.

4.3 Biodiversity effects on C and N cycles

Biodiversity, including plant diversity, increases drastically after conversion from lawn to meadow (Venn and Kotze, 2014; Chollet et al., 2018; Norton et al., 2019). Thus, we wanted to understand how plant diversity could affect the SOC and the

575 GHG fluxes at our sites. However, contrary to what was revealed in other studies (Fornara and Tilman, 2008; Lange et al., 2015), we did not find any link between the plant diversity and the C and N cycles, i.e. TER, CH₄, N₂O fluxes and C and N soil contents. Indeed, a large variety of plants could explain a higher rate of TER (Dias et al., 2010) and could facilitate more

N and C storage in the soil (Fornara and Tilman, 2008; Oelmann et al., 2011; Mueller et al., 2013; Cong et al., 2014; Lange et al., 2015). Nevertheless, Wei et al. (2017) demonstrated that with high plant functional group diversity, instead of species

580 diversity, the nitrate pool and the N mineralization rate were lowered. Mueller et al. (2013) also found that high diversity enhances N transformation and NH_4^+ pool, but a too high plant diversity could also have the opposite effect. One of the issues in our study could be that we studied the influence of diversity with only a one-year dataset in order to include the satellite as well as the intensive sites. The second issue may be that we used the SOC and SON instead of their accumulation over the years, because a three-year period is not enough to appreciate a C or N accumulation in the soil, where the changes

585 happen slowly, i.e. a changing rate lower than 2% per year (Fornara and Tilman, 2008), whereas the standing pools of C and N are reflecting also historical land use.

To go further into the diversity, we tested the link of different plant categories, i.e. grasses, legumes, forbs, trees, sedges, horsetails and mosses, on the C and N cycles. As expected, according to our analysis, TER increased with most of the plant categories and CH_4 was connected to hygrophytes, such as horsetails and mosses. Even though some of the fluxes were

590 according to the analysis linked to trees, sedges, horsetails and mosses, it would be beneficial to validate the results with a broader dataset since mosses and sedges were present in only one site, horsetails in two sites and trees saplings were surveyed in only three sites, whereas there were 8 sites included in the studies. Nevertheless, we showed that SOC increases with forbs, of which the proportion is higher in meadows. Hence, the meadows could store more carbon than lawns as also: (1) because of the transformation, some SOC could have been incorporated into the soil; (2) meadows could have created

595 more litter that enriched the soil in carbon; and (3) with a deep and strong root system, forbs could have allocated more carbon into the soil. However, such an increase in soil carbon was not revealed by the plant diversity analysis or supported by the flux analysis. Furthermore, the SON model was not significant according to the R-squared, but SON was slightly related to grasses and forbs, and not to legumes; however, in the transformed meadows, the proportion of legumes was rather low.

600 Some other studies have also tried to estimate the correlation between plant functional type and soil characteristics, by studying C3 and C4 grasses and legumes (Fornara and Tilman, 2008; Yang et al., 2019). Fornara and Tilman (2008) estimated that C4 grasses may increase soil carbon accumulation by 193%, and legumes by 522%. Moreover, even though legumes did not appear to be one of the significant groups in our SOC model and negatively connected to C/N ratio, legumes are known to improve the soil N availability and the litter quality by reducing the C/N ratio (Fornara and Tilman, 2008;

605 Yang et al., 2019). Thus, plant functional types undoubtedly impact the C and N cycles, but to get a stronger conclusion on the impact of the functional types on carbon and nitrogen dynamics, it would be necessary to study a higher number of sites and also compare chosen mixtures of plants on ground with the same soil properties.

5 Conclusions

In order to slow down the biodiversity loss, cities around the world are considering converting their lawns into meadows.

610 Another priority is to mitigate climate change and achieve carbon neutrality. In this study, we focused on urban grasslands from a climate and biodiversity perspective by studying maintained lawns in comparison with mature and newly transformed meadows in northern Europe at the border between the boreal and temperate zones. The transformation from lawns to meadows did not demonstrate any negative climate effects in terms of ecosystem respiration, CH_4 and N_2O fluxes. Meadows do increase biodiversity, but we found that they do not increase carbon sequestration compared with lawns on an annual

615 scale. Nevertheless, in a climate warming perspective, with more frequent extreme events, meadows resist drought events better than lawns and are better able, at least in the short term, to adapt cities to extreme drought events induced by climate change; nonetheless, it would be necessary to check this result at a larger scale, and investigate the overall resilience with longer time series dataset, to help stakeholders and city planners to make the right decisions to optimize land-use. Thus,

considering biodiversity, climate warming and carbon neutrality, it is necessary to find the right trade-off between lawns and

620   meadows in cities. Regarding the plant diversity, the species richness does not seem to affect significantly the C and N cycles, even though some vegetation categories seem to be correlated to specific C and N status. Nevertheless, as this analysis was done with only one-year dataset, it would be necessary to investigate with more sites, on the link between plants and C and N cycle. Moreover, it would be beneficial to further study the carbon storage process and its longevity, as well as the biodiversity dynamics during transformation from lawns to meadows or drought resilience processes, and to consider the

625   social aspects of the conversion of lawns to meadows.

Data availability

The data used in the manuscript can be downloaded from Finnish Meteorological data storage: http://hdl.handle.net/11304/9a597a75-6f3b-48ce-b3e6-d23598817a5b, https://doi.org/10.23728/fmi-b2share.6cfb9e97b72648d6ad57f02c210fe042 (Trémeau et al., 2023).

630   **Supplement link**

Author contributions

LK, BO, EK and JT designed the research; BO, EK and JT participated in the data collection; HV, LK, EK and JT participated in the flux calculations; JT conducted the statistical data analyses; LB performed the JSBACH simulations; all of the authors participated in writing the paper.

635   **Competing interests**

The authors declare that they have no conflict of interest.

Acknowledgements

References

Allaire, S. E., Dufour-L'Arrivée, C., Lafond, J. A., Lalancette, R., and Brodeur, J.: Carbon dioxide emissions by urban turfgrass areas, Can. J. Soil. Sci., 88, 529–532, https://doi.org/10.4141/CJSS07043, 2008.

655 Bates, D., Mächler, M., Bolker, B., and Walker, S.: Fitting Linear Mixed-Effects Models Using lme4, Journal of Statistical Software, 67, 1–48, https://doi.org/10.18637/jss.v067.i01, 2015.

Beguería, S., Vicente-Serrano, S. M., Reig, F., and Latorre, B.: Standardized precipitation evapotranspiration index (SPEI) revisited: parameter fitting, evapotranspiration models, tools, datasets and drought monitoring, International Journal of Climatology, 34, 3001–3023, https://doi.org/10.1002/joc.3887, 2014.

660 Belmeziti, A., Cherqui, F., and Kaufmann, B.: Improving the multi-functionality of urban green spaces: Relations between components of green spaces and urban services, Sustainable Cities and Society, 43, 1–10, https://doi.org/10.1016/j.scs.2018.07.014, 2018.

Bernath-Plaisted, J. S., Ribic, C. A., Hills, W. B., Townsend, P. A., and Zuckerberg, B.: Microclimate complexity in temperate grasslands: implications for conservation and management under climate change, Environ. Res. Lett., 18, 064023, 665 https://doi.org/10.1088/1748-9326/acd4d3, 2023.

Bezyk, Y., Dorodnikov, M., Grzelka, A., and Nych, A.: Characteristics of temporal variability of urban ecosystem-atmosphere CO_2, CH_4, and N_2O fluxes, E3S Web Conf., 44, 00013, https://doi.org/10.1051/e3sconf/20184400013, 2018.

Böttcher, K., Markkanen, T., Thum, T., Aalto, T., Aurela, M., Reick, C. H., Kolari, P., Arslan, A. N., and Pulliainen, J.: Evaluating Biosphere Model Estimates of the Start of the Vegetation Active Season in Boreal Forests by Satellite 670 Observations, Remote Sensing, 8, 580, https://doi.org/10.3390/rs8070580, 2016.

Bretzel, F., Gaetani, M., Vannucchi, F., Caudai, C., Grossi, N., Magni, S., Caturegli, L., and Volterrani, M.: A multifunctional alternative lawn where warm-season grass and cold-season flowers coexist, Landscape Ecol Eng, 16, 307–317, https://doi.org/10.1007/s11355-020-00423-w, 2020.

Capdevila, P., Stott, I., Oliveras Menor, I., Stouffer, D. B., Raimundo, R. L. G., White, H., Barbour, M., and Salguero-675 Gómez, R.: Reconciling resilience across ecological systems, species and subdisciplines, Journal of Ecology, 109, 3102–3113, https://doi.org/10.1111/1365-2745.13775, 2021.

Chaudron, C., Mazalová, M., Kuras, T., Malenovský, I., and Mládek, J.: Introducing ecosystem engineers for grassland biodiversity conservation: A review of the effects of hemiparasitic Rhinanthus species on plant and animal communities at multiple trophic levels, Perspectives in Plant Ecology, Evolution and Systematics, 52, 125633, 680 https://doi.org/10.1016/j.ppees.2021.125633, 2021.

Chen, X., Chen, H. Y. H., Chen, C., Ma, Z., Searle, E. B., Yu, Z., and Huang, Z.: Effects of plant diversity on soil carbon in diverse ecosystems: a global meta-analysis, Biological Reviews, 95, 167–183, https://doi.org/10.1111/brv.12554, 2020.

Chollet, S., Brabant, C., Tessier, S., and Jung, V.: From urban lawns to urban meadows: Reduction of mowing frequency increases plant taxonomic, functional and phylogenetic diversity, Landscape and Urban Planning, 180, 121–124, 685 https://doi.org/10.1016/j.landurbplan.2018.08.009, 2018.

Cong, W.-F., van Ruijven, J., Mommer, L., De Deyn, G. B., Berendse, F., and Hoffland, E.: Plant species richness promotes soil carbon and nitrogen stocks in grasslands without legumes, Journal of Ecology, 102, 1163–1170, https://doi.org/10.1111/1365-2745.12280, 2014.

De Boeck, H. J., Lemmens, C. M. H. M., Bossuyt, H., Malchair, S., Carnol, M., Merckx, R., Nijs, I., and Ceulemans, R.: 690 How do climate warming and plant species richness affect water use in experimental grasslands?, Plant Soil, 288, 249–261, https://doi.org/10.1007/s11104-006-9112-5, 2006.

De Keersmaecker, W., van Rooijen, N., Lhermitte, S., Tits, L., Schaminée, J., Coppin, P., Honnay, O., and Somers, B.: Species-rich semi-natural grasslands have a higher resistance but a lower resilience than intensively managed agricultural grasslands in response to climate anomalies, Journal of Applied Ecology, 53, 430–439, https://doi.org/10.1111/1365-695 2664.12595, 2016.

Dias, A. T. C., van Ruijven, J., and Berendse, F.: Plant species richness regulates soil respiration through changes in productivity, Oecologia, 163, 805–813, https://doi.org/10.1007/s00442-010-1569-5, 2010.

Elonen, P.: Particle-size analysis of soil, Suomen maataloustieteellinen seura, 122, 1971.

European Commission: Proposal for a regulation of the european parlament and the concil on nature restoration, https://doi.org/10.5281/ZENODO.5657041, 2022.

Farquhar, G. D., von Caemmerer, S., and Berry, J. A.: A biochemical model of photosynthetic CO_2 assimilation in leaves of C3 species, Planta, 149, 78–90, https://doi.org/10.1007/BF00386231, 1980.

Finnish Meteorological Institute. Download observations: https://en.ilmatieteenlaitos.fi/download-observations, last access: 21 April 2023.

Fischer, L. K., Lippe, M. von der, Rillig, M. C., and Kowarik, I.: Creating novel urban grasslands by reintroducing native species in wasteland vegetation, Biological Conservation, 159, 119–126, https://doi.org/10.1016/j.biocon.2012.11.028, 2013.

Fornara, D. A. and Tilman, D.: Plant functional composition influences rates of soil carbon and nitrogen accumulation, Journal of Ecology, 96, 314–322, https://doi.org/10.1111/j.1365-2745.2007.01345.x, 2008.

GADM. Maps and data. Ver 4.1: https://gadm.org/index.html, last access: 21 April 2023.

Hagemann, S. and Stacke, T.: Impact of the soil hydrology scheme on simulated soil moisture memory, Clim Dyn, 44, 1731–1750, https://doi.org/10.1007/s00382-014-2221-6, 2015.

Hiller, R. V., McFadden, J. P., and Kljun, N.: Interpreting CO_2 Fluxes Over a Suburban Lawn: The Influence of Traffic Emissions, Boundary-Layer Meteorol, 138, 215–230, https://doi.org/10.1007/s10546-010-9558-0, 2011.

Hossain, M. L., Li, J., Hoffmann, S., and Beierkuhnlein, C.: Biodiversity showed positive effects on resistance but mixed effects on resilience to climatic extremes in a long-term grassland experiment, Science of The Total Environment, 827, 154322, https://doi.org/10.1016/j.scitotenv.2022.154322, 2022.

Hundertmark, W. J., Lee, M., Smith, I. A., Bang, A. H. Y., Chen, V., Gately, C. K., Templer, P. H., and Hutyra, L. R.: Influence of landscape management practices on urban greenhouse gas budgets, Carbon Balance and Management, 16, 1, https://doi.org/10.1186/s13021-020-00160-5, 2021.

Institute of Atmospheric Research. SmartSMEAR - Download: https://smear.avaa.csc.fi/download, last access: 21 April 2023.

IPCC: Climate Change 2022: Impacts, Adaptation, and Vulnerability. Contribution of Working Group II to the Sixth Assessment Report of the Intergovernmental Panel on Climate Change, IPCC, 2022.

Järvi, L., Hannuniemi, H., Hussein, T., Junninen, H., Aalto, P., Hillamo, R., Mäkelä, T., Keronen, P., Siivola, E., Vesala, T., and Kulmala, M.: The urban measurement station SMEAR III: Continuous monitoring of air pollution and surface–atmosphere interactions in Helsinki, Finland, 14, 2009.

Jokinen, P., Pirinen, P., Kaukoranta, J.-P., Kangas, A., Alenius, P., Eriksson, P., Johansson, M., and Wilkman, S.: Climatological and oceanographic statistics of Finland 1991–2020, Finnish Meteorological Institute, https://doi.org/10.35614/isbn.9789523361485, 2021.

Jung, E.-Y., Gaviria, J., Sun, S., and Engelbrecht, B. M. J.: Comparative drought resistance of temperate grassland species: testing performance trade-offs and the relation to distribution, Oecologia, 192, 1023–1036, https://doi.org/10.1007/s00442-020-04625-9, 2020.

Kohl, L., Koskinen, M., Rissanen, K., Haikarainen, I., Polvinen, T., Hellén, H., and Pihlatie, M.: Technical note: Interferences of volatile organic compounds (VOCs) on methane concentration measurements, Biogeosciences, 16, 3319–3332, https://doi.org/10.5194/bg-16-3319-2019, 2019.

Kose, M., Heinsoo, K., Kaljund, K., and Tali, K.: Twenty years of Baltic Boreal coastal meadow restoration: has it been long enough?, Restoration Ecology, 29, e13266, https://doi.org/10.1111/rec.13266, 2021.

Kottek, M., Grieser, J., Beck, C., Rudolf, B., and Rubel, F.: World Map of the Köppen-Geiger climate classification updated, metz, 15, 259–263, https://doi.org/10.1127/0941-2948/2006/0130, 2006.

Lampinen, J., Tuomi, M., Fischer, L. K., Neuenkamp, L., Alday, J. G., Bucharova, A., Cancellieri, L., Casado-Arzuaga, I., Čeplová, N., Cerveró, L., Deák, B., Eriksson, O., Fellowes, M. D. E., de Manuel, B. F., Filibeck, G., González-Guzmán, A., Hinojosa, M. B., Kowarik, I., Lumbierres, B., Miguel, A., Pardo, R., Pons, X., Rodríguez-García, E., Schröder, R., Sperandii, M. G., Unterweger, P., Valkó, O., Vázquez, V., and Klaus, V. H.: Acceptance of near-natural greenspace

management relates to ecological and socio-cultural assigned values among European urbanites, Basic and Applied Ecology,
50, 119–131, https://doi.org/10.1016/j.baae.2020.10.006, 2021.

Lane, I. G., Wolfin, J., Watkins, E., and Spivak, M.: Testing the Establishment of Eight Forbs in Mowed Lawns of Hard
Fescue (Festuca brevipila) for Use in Pollinator Conservation in: HortScience Volume 54 Issue 12 (2019), 2019.

Lange, M., Eisenhauer, N., Sierra, C. A., Bessler, H., Engels, C., Griffiths, R. I., Mellado-Vázquez, P. G., Malik, A. A., Roy,
J., Scheu, S., Steinbeiss, S., Thomson, B. C., Trumbore, S. E., and Gleixner, G.: Plant diversity increases soil microbial
activity and soil carbon storage, Nat Commun, 6, 6707, https://doi.org/10.1038/ncomms7707, 2015.

Lerman, S. B. and Contosta, A. R.: Lawn mowing frequency and its effects on biogenic and anthropogenic carbon dioxide
emissions, Landscape and Urban Planning, 182, 114–123, https://doi.org/10.1016/j.landurbplan.2018.10.016, 2019.

Loreau, M. and Hector, A.: Partitioning selection and complementarity in biodiversity experiments, Nature, 412, 72–76,
https://doi.org/10.1038/35083573, 2001.

Mueller, K. E., Hobbie, S. E., Tilman, D., and Reich, P. B.: Effects of plant diversity, N fertilization, and elevated carbon
dioxide on grassland soil N cycling in a long-term experiment, Global Change Biology, 19, 1249–1261,
https://doi.org/10.1111/gcb.12096, 2013.

Muller, S., Dutoit, T., Alard, D., and Grévilliot, F.: Restoration and Rehabilitation of Species-Rich Grassland Ecosystems in
France: a Review, Restoration Ecology, 6, 94–101, https://doi.org/10.1046/j.1526-100x.1998.06112.x, 1998.

Muñoz-Sabater, J., Dutra, E., Agustí-Panareda, A., Albergel, C., Arduini, G., Balsamo, G., Boussetta, S., Choulga, M.,
Harrigan, S., Hersbach, H., Martens, B., Miralles, D. G., Piles, M., Rodríguez-Fernández, N. J., Zsoter, E., Buontempo, C.,
and Thépaut, J.-N.: ERA5-Land: a state-of-the-art global reanalysis dataset for land applications, Earth System Science Data,
13, 4349–4383, https://doi.org/10.5194/essd-13-4349-2021, 2021.

National Land Survey of Finland. Topographic Database: http://www.maanmittauslaitos.fi/en/maps-and-spatial-data/expert-
users/product-descriptions/topographic-database, last access: 21 April 2023.

Nevalainen, O.: ollinevalainen/satellitetools: v1.0.0, https://doi.org/10.5281/zenodo.5993292, 2022.

Nevalainen, O., Niemitalo, O., Fer, I., Juntunen, A., Mattila, T., Koskela, O., Kukkamäki, J., Höckerstedt, L., Mäkelä, L.,
Jarva, P., Heimsch, L., Vekuri, H., Kulmala, L., Stam, Å., Kuusela, O., Gerin, S., Viskari, T., Vira, J., Hyväluoma, J.,
Tuovinen, J.-P., Lohila, A., Laurila, T., Heinonsalo, J., Aalto, T., Kunttu, I., and Liski, J.: Towards agricultural soil carbon
monitoring, reporting, and verification through the Field Observatory Network (FiON), Geoscientific Instrumentation,
Methods and Data Systems, 11, 93–109, https://doi.org/10.5194/gi-11-93-2022, 2022.

Norton, B. A., Bending, G. D., Clark, R., Corstanje, R., Dunnett, N., Evans, K. L., Grafius, D. R., Gravestock, E., Grice, S.
M., Harris, J. A., Hilton, S., Hoyle, H., Lim, E., Mercer, T. G., Pawlett, M., Pescott, O. L., Richards, J. P., Southon, G. E.,
and Warren, P. H.: Urban meadows as an alternative to short mown grassland: effects of composition and height on
biodiversity, Ecological Applications, 29, e01946, https://doi.org/10.1002/eap.1946, 2019.

Oelmann, Y., Buchmann, N., Gleixner, G., Habekost, M., Roscher, C., Rosenkranz, S., Schulze, E.-D., Steinbeiss, S.,
Temperton, V. M., Weigelt, A., Weisser, W. W., and Wilcke, W.: Plant diversity effects on aboveground and belowground
N pools in temperate grassland ecosystems: Development in the first 5 years after establishment, Global Biogeochemical
Cycles, 25, https://doi.org/10.1029/2010GB003869, 2011.

Patrignani, A. and Ochsner, T. E.: Canopeo: A Powerful New Tool for Measuring Fractional Green Canopy Cover,
Agronomy Journal, 107, 2312–2320, https://doi.org/10.2134/agronj15.0150, 2015.

Pavelka, M., Acosta, M., Kiese, R., Altimir, N., Brümmer, C., Crill, P., Darenova, E., Fuß, R., Gielen, B., Graf, A.,
Klemedtsson, L., Lohila, A., Longdoz, B., Lindroth, A., Nilsson, M., Jiménez, S. M., Merbold, L., Montagnani, L., Peichl,
M., Pihlatie, M., Pumpanen, J., Ortiz, P. S., Silvennoinen, H., Skiba, U., Vestin, P., Weslien, P., Janous, D., and Kutsch, W.:
Standardisation of chamber technique for CO2, N2O and CH4 fluxes measurements from terrestrial ecosystems,
International Agrophysics, 32, 569–587, https://doi.org/10.1515/intag-2017-0045, 2018.

Poeplau, C., Marstorp, H., Thored, K., and Kätterer, T.: Effect of grassland cutting frequency on soil carbon storage – a case
study on public lawns in three Swedish cities, SOIL, 2, 175–184, https://doi.org/10.5194/soil-2-175-2016, 2016.

Pörtner, H.-O., Scholes, R. J., Agard, J., Archer, E., Arneth, A., Bai, X., Barnes, D., Burrows, M., Chan, L., Cheung, W. L.
(William), Diamond, S., Donatti, C., Duarte, C., Eisenhauer, N., Foden, W., Gasalla, M. A., Handa, C., Kätterer, T., Hoegh-
Guldberg, O., Ichii, K., Jacob, U., Insarov, G., Kiessling, W., Leadley, P., Leemans, R., Levin, L., Lim, M., Maharaj, S.,

Managi, S., Marquet, P. A., McElwee, P., Midgley, G., Oberdorff, T., Obura, D., Osman Elasha, B., Pandit, R., Pascual, U., Pires, A. P. F., Popp, A., Reyes-García, V., Sankaran, M., Settele, J., Shin, Y.-J., Sintayehu, D. W., Smith, P., Steiner, N., Strassburg, B., Sukumar, R., Trisos, C., Val, A. L., Wu, J., Aldrian, E., Parmesan, C., Pichs-Madruga, R., Roberts, D. C., Rogers, A. D., Díaz, S., Fischer, M., Hashimoto, S., Lavorel, S., Wu, N., and Ngo: Scientific outcome of the IPBES-IPCC co-sponsored workshop on biodiversity and climate change, Zenodo, https://doi.org/10.5281/ZENODO.4659158, 2021.

Reick, C. H., Raddatz, T., Brovkin, V., and Gayler, V.: Representation of natural and anthropogenic land cover change in MPI-ESM, Journal of Advances in Modeling Earth Systems, 5, 459–482, https://doi.org/10.1002/jame.20022, 2013.

Riikonen, A. and Karilas, A.: Maaherranpuiston OmaStadi-niitty, Prosessin kuvaus ja niityn kehittymisen seuranta - VÄLIRAPORTTI 2021 [Maaherranpuisto's OmaStadi meadow, Description of the process and monitoring of the development of the meadow - INTERIM REPORT 2021, in Finnish], Sitowise, 2021.

Ruimy, A., Jarvis, P. G., Baldocchi, D. D., and Saugier, B.: CO_2 Fluxes over Plant Canopies and Solar Radiation: A Review, in: Advances in Ecological Research, vol. 26, edited by: Begon, M. and Fitter, A. H., Academic Press, 1–68, https://doi.org/10.1016/S0065-2504(08)60063-X, 1995.

Ryhti, K., Kulmala, L., Pumpanen, J., Isotalo, J., Pihlatie, M., Helmisaari, H.-S., Leppälammi-Kujansuu, J., Kieloaho, A.-J., Bäck, J., and Heinonsalo, J.: Partitioning of forest floor CO_2 emissions reveals the belowground interactions between different plant groups in a Scots pine stand in southern Finland, Agricultural and Forest Meteorology, 297, 108266, https://doi.org/10.1016/j.agrformet.2020.108266, 2021.

Southon, G. E., Jorgensen, A., Dunnett, N., Hoyle, H., and Evans, K. L.: Biodiverse perennial meadows have aesthetic value and increase residents' perceptions of site quality in urban green-space, Landscape and Urban Planning, 158, 105–118, https://doi.org/10.1016/j.landurbplan.2016.08.003, 2017.

Thienelt, T. S. and Anderson, D. E.: Estimates of energy partitioning, evapotranspiration, and net ecosystem exchange of CO_2 for an urban lawn and a tallgrass prairie in the Denver metropolitan area under contrasting conditions, Urban Ecosyst, 24, 1201–1220, https://doi.org/10.1007/s11252-021-01108-4, 2021.

Thompson, K., Hodgson, J. G., Smith, R. M., Warren, P. H., and Gaston, K. J.: Urban domestic gardens (III): Composition and diversity of lawn floras, Journal of Vegetation Science, 15, 373–378, https://doi.org/10.1111/j.1654-1103.2004.tb02274.x, 2004.

Tilman, D., Lehman, C. L., and Thomson, K. T.: Plant diversity and ecosystem productivity: Theoretical considerations, Proceedings of the National Academy of Sciences, 94, 1857–1861, https://doi.org/10.1073/pnas.94.5.1857, 1997.

Trémeau, J., Karvinen, E., and Olascoaga, B.: Fluxes and plant diversity data in urban grasslands, https://doi.org/10.23728/fmi-b2share.6cfb9e97b72648d6ad57f02c210fe042, 2023.

Venn, S. and Kotze, J.: Benign neglect enhances urban habitat heterogeneity: Responses of vegetation and carabid beetles (Coleoptera: Carabidae) to the cessation of mowing of park lawns, European Journal of Entomology, 111, 703–714, https://doi.org/10.14411/eje.2014.089, 2014.

Vicente-Serrano, S. M., Beguería, S., and López-Moreno, J. I.: A Multiscalar Drought Index Sensitive to Global Warming: The Standardized Precipitation Evapotranspiration Index, Journal of Climate, 23, 1696–1718, https://doi.org/10.1175/2009JCLI2909.1, 2010.

Viherympäristöliitto. ABC-Vastaavuus: https://www.vyl.fi/ohjeet/kunnossapitoluokitus/vastaavuus/, last access: 21 April 2023.

Vogel, A., Scherer-Lorenzen, M., and Weigelt, A.: Grassland Resistance and Resilience after Drought Depends on Management Intensity and Species Richness, PLOS ONE, 7, e36992, https://doi.org/10.1371/journal.pone.0036992, 2012.

Waldén, E. and Lindborg, R.: Long Term Positive Effect of Grassland Restoration on Plant Diversity - Success or Not?, PLOS ONE, 11, e0155836, https://doi.org/10.1371/journal.pone.0155836, 2016.

Wang, Q., Zeng, J., Qi, J., Zhang, X., Zeng, Y., Shui, W., Xu, Z., Zhang, R., Wu, X., and Cong, J.: A multi-scale daily SPEI dataset for drought characterization at observation stations over mainland China from 1961 to 2018, Earth System Science Data, 13, 331–341, https://doi.org/10.5194/essd-13-331-2021, 2021.

Wastian, L., Unterweger, P. A., and Betz, O.: Influence of the reduction of urban lawn mowing on wild bee diversity (Hymenoptera, Apoidea), JHR, 49, 51–63, https://doi.org/10.3897/JHR.49.7929, 2016.

840 Watson, C. J., Carignan-Guillemette, L., Turcotte, C., Maire, V., and Proulx, R.: Ecological and economic benefits of low-intensity urban lawn management, Journal of Applied Ecology, 57, 436–446, https://doi.org/10.1111/1365-2664.13542, 2020.

Wei, X., Reich, P. B., Hobbie, S. E., and Kazanski, C. E.: Disentangling species and functional group richness effects on soil N cycling in a grassland ecosystem, Global Change Biology, 23, 4717–4727, https://doi.org/10.1111/gcb.13757, 2017.

Yang, Y., Tilman, D., Furey, G., and Lehman, C.: Soil carbon sequestration accelerated by restoration of grassland
845 biodiversity, Nat Commun, 10, 718, https://doi.org/10.1038/s41467-019-08636-w, 2019.

Zirkle, G., Lal, R., and Augustin, B.: Modeling Carbon Sequestration in Home Lawns, HortScience, 46, 808–814, https://doi.org/10.21273/HORTSCI.46.5.808, 2011.